



Research papers

Sediment transport and morphodynamical modeling on the estuaries and coastal zone of the Vietnamese Mekong Delta



Le Xuan Tu^{a,b}, Vo Quoc Thanh^{a,c}, Johan Reyns^{a,d}, Song Pham Van^e, Duong Tran Anh^{e,f,*}, Thanh Duc Dang^g, Dano Roelvink^{a,d}

^a IHE Delft Institute of Water Education, the Netherlands

^b Southern Institute of Water Resource Research, Ho Chi Minh City, Viet Nam

^c Can Tho University, Viet Nam

^d Deltares, Delft, the Netherlands

^e Environment, Water and Climate Change Adaptation Research Group, Vietnamese-German University, Binh Duong Province, Viet Nam

^f Institute of Hydraulic and Water Resources Engineering, Technical University of Munich, Germany

^g Pillar of Engineering Systems and Design, Singapore University of Technology and Design, Singapore

ARTICLE INFO

Keywords:

Morphodynamics
Sediment transport
Estuary
Coastal zone
Mekong delta

ABSTRACT

The estuaries and coastal zones of the Vietnamese Mekong Delta located at the end of the Mekong Basin are susceptible to a large variety of natural threats and human interventions such as upstream dam construction, climate change and sea level rise. In this study, we investigated sediment dynamics and morphodynamic changes in the Mekong estuaries and coastal zone, using a well-calibrated Delft3D-4 model for a 10-years period simulation. For the first time, the impacts of different drivers were distinguished to guide future adaptation strategies and policies. Our investigations pointed out that the influences of upstream sediment reduction and large-scale sand extraction would cause substantial modifications in the subaqueous delta region. Besides human-induced impacts, modeling results also showed that the sediment volume and spatial distribution changed through the simulated period according to monsoonal variation. The influence of each driver, however, not only varied in space but also time. In the flood season, the Mekong and Bassac Rivers provided a large amount of sediment (more than 90%) that was deposited on the delta front due to coastal processes. The sediment quantity transported along the coastline changed with the monsoon and was in a dominantly south-west direction due to the northeast monsoon, especially in November, December and January. As a natural process, in the estuarine region, erosion and deposition occurred alternately, but the south-west coast region (belonging to the Ca Mau peninsula) was dominated by erosion. This is because of the formation of sand bars in front of the Bassac estuaries, which influences the capacity of sediment transportation to the south-west. Consequently, navigation capacity will reduce significantly in the estuaries and coastline erosion in the Ca Mau peninsula leads to substantial loss of houses and assets of local people. Urgent actions such as stopping sand mining or modifying dam designs are needed to sustain the delta coastline.

1. Introduction

River deltas are important to human activities and ecosystems because they are extremely fertile lands with abundant water and diverse vegetation. While the formation of river deltas is considerably slow, alluvium deposition processes have been increasingly altered caused by human activities. Massive damming and sand excavation are degrading and threatening the existence of river deltas around the world (Arias et al., 2019; Hecht et al., 2019; Milliman and Farnsworth, 2011).

When international concern for the survival of deltas grows, the

Mekong river delta, the world's third largest delta, which is densely populated, is considered as Southeast Asia's most important food basket, is increasingly affected by human activities and exposed to subsidence and coastal erosion (Ogston et al., 2017). Recently, the Mekong basin has become one of the most active regions for hydro-power development in the world. According to MRC (2011), there are totally over 130 existing and planned dams in the Mekong Basin which cause various negative impacts on hydrology and sediment flows in the downstream and the delta (Hecht et al., 2019). Upstream dams may trap more than 90% of terrigenous materials which would otherwise be

* Corresponding author. Technical University of Munich, Germany. ,

E-mail addresses: tran.duong@tum.de, trananhduong1981@gmail.com (D.T. Anh).

<https://doi.org/10.1016/j.csr.2019.07.015>

Received 23 January 2019; Received in revised form 20 July 2019; Accepted 23 July 2019

Available online 26 July 2019

0278-4343/ © 2019 Elsevier Ltd. All rights reserved.

transported to the lower river system (Kondolf et al., 2014; Manh et al., 2015). Inside the floodplains, large-scale commercial sand mining from channels aggravated morphology changes and coastal erosion in recent years (Anthony et al., 2015). Manh et al. (2014) modelled sediment transportation in the Vietnamese Mekong Delta by the DHI-MIKE 11 model and found that sediment was also trapped during the flood season due to dyke construction. All human activities have significantly influenced sediment dynamics and morphology of the estuary and coastal zone, and further threaten the stability of livelihoods and settlement of over 10 millions in the Mekong Delta.

Sediment transport and morphological changes of the Mekong estuaries has been scrutinized with significant efforts and advanced models. Wolanski et al. (1998, 1996) and Hein et al. (2013) conducted studies to quantify sediment transport processes in the delta, but they focused on short-term sediment transport and local morphodynamical changes. The lack of long-term measurement hindered their efforts in providing a thorough view of sediment dynamics in the region. Recently, Hein et al. (2013) showed severe erosion along the south coast of the delta caused by strong ocean currents along the coasts and wave action. Hein et al. (2013) and Unverricht et al. (2014), however, focused on the subaqueous delta, i.e. the seaward area of the shoreline. For the inland part of the delta, numerous studies on sediment transport were carried out by Hung et al. (2014a, 2014b), Manh et al. (2014, 2015), Nowacki et al. (2015), Vinh et al. (2016), and Xing et al. (2017). Nowacki et al. (2015) found that sediment flux patterns are strongly related to the tidal processes as well as river discharge. Moreover, to understand seasonal wind and wave impacts on sediment transport in the coast of VMD, Vinh et al. (2016) carried out a study using the Delft3D model to simulate sediment transports from Can Tho, My Thuan and Soai Rap to the Vietnamese East Sea (also called the South China Sea). The result of their study provided an estimation in the quantity of sediment transported along the coast at several cross-shore sections and the roles of river discharge and suspended sediment supply variation over the seasons. Thanh et al. (2017) studied suspended sediment dynamics on the delta shelf and presented more clearly seasonal suspended sediment dynamics influenced by salt concentration, wave and sediment properties. Dang et al. (2018b), Wackerman et al. (2017), Anthony et al. (2017) and Heege et al. (2014) studied sediment dynamics in the Mekong Delta by remote sensing, and DeMaster et al. (2017) employed radiochemical tracers to determine rates of sediment accumulation on the Mekong shelf. However, these techniques can only explain past sediment dynamics. Recently, Marchesiello et al. (2019) studied the dynamics of mud in the region using the Coastal and Regional Ocean Community model (CROCO). Nevertheless, they ignored the influence of alongshore currents, so as mud particles settle around the river mouths but not travel further to the Ca Mau cape. None of them studied the impact of human influences in the complex environment of the mixed impacts of tides and waves in a long-term process.

This study aims to investigate the effects of salinity, tides and winds on long-term sediment transport from the estuary to the sea through field campaigns and considers the influences of human activities via a well-calibrated hydro-morphological model. We also tried to derive the long-term relationship between hydrodynamics, sediment transport and bed level evolution. The result from this study would provide an overview for planning authorities dealing with sediment management, navigation and coastal zone management. This would be also an example for similar river deltas around the world under effects of human intervention.

2. Methodology and data collection

2.1. Methodology

We used the Delft3D–Flow module coupled with the Delft3D–Wave module and a sediment transport model in this study. This approach is widely applied to simulate hydrodynamics, sediment transport, and

morphology in river and coastal areas around the world (Duong et al., 2012; Garcia et al., 2015; Lu et al., 2015; van der Wegen et al., 2011).

Upstream boundaries data were obtained from the national hydrological stations which are further discussed below. Water level boundaries (sea levels) were based on tidal prediction with astronomical components (M2, S2, N2, K2, K1, O1, P1 and Q1) in six different sections from the TPXO 7.2 global tidal model (Egbert and Erofeeva, 2002). The Neumann astronomical boundary conditions were applied to allow the free development of cross-shore water level slopes and flow profiles due to effects of tides, Coriolis, wind and waves. Parameters to calibrate the model included bed roughness, shear stresses for erosion and deposition, and the settling velocity of sediment particles. We used the years 2009 and 2010 because these two years included the lowest flood year (2010) and a year with larger than average floods (2009) in the 94-year record (1920–2013). The defined water year started on 01-June (starting of the flood season) and ended on 31-May of the next year (the end of the dry season), to include the peak discharges that occurred in November and the lowest discharge in April. Through this selection, a wide range of possible hydrological events and associated sediment dynamics in the estuary were covered.

2.2. Bathymetry

The Mekong River Delta in Vietnam is at the end of the Mekong Basin – a transboundary river basin shared by China, Myanmar, Thailand, Laos, Cambodia and Vietnam. In the delta, the river divides into two branches, the Mekong and Bassac Rivers. The study region covers two areas, including the riverine estuaries and the shelf. Moving along the coast from the North to the South parts of the delta, there are eight main estuaries which are Soai Rap, Cua Dai, Cua Tieu, Ham Luong, Co Chien, Cung Hau, Dinh An, and Tran De. The bathymetry of the river system was interpolated from cross sections (the distance of 0.5–1.2 km) surveyed in 2008–2010 by the Southern Institute of Water Resource Research (SIWRR), Viet Nam. The estuarine bathymetry was measured during the period 2009–2010 by SIWRR. The sea shelf bathymetry which was investigated in 2008–2010 was collected from the Ministry of Resources and Environment, Viet Nam.

In this study, the bathymetry of the model was updated continuously while a morphological acceleration factor ('morfac'), which significantly improved the capability to carry out longer-term simulations, was applied as in Roelvink (2006). This technique is introduced for long-term morphodynamic modeling, aiming to accelerate the simulation while keeping the time-variation of discharge, wave and climate within a year. The time-series of the input conditions over a year were squeezed by a factor equalling to the morphological factor (MORFAC). MORFAC is set to 25 in this case which is applied worldwide (see Roelvink (2006) for more detail); this means that a year was reduced to a representative hydrodynamic period of 365/25 days, roughly two weeks.

Changes of bathymetry during modeling could influence hydrodynamic results. Additionally, we considered human activities, including sand mining, dredging, or constructing groins at the coastline, which lead to sharp changes in hydrodynamic characteristics.

2.3. Hydrological and sediment data

The time series of discharges and suspended sediment concentration (SSC) measured at Can Tho and My Thuan were used for the upstream boundary conditions (Fig. 1). The river discharges were measured every hour at the Can Tho and My Thuan stations. The river discharges at the Soai Rap station were extracted from the result of the DHI-MIKE model for the Sai Gon and Dong Nai rivers system which was set up and calibrated by SIWRR as in Manh et al. (2014). SSC at Soai Rap was set at 0.2 kg/m³ which was the annual mean of observed values measured by SIWRR. Soai Rap, which is the outlet of the Sai Gon – Dong Nai river system, has much lower discharge compared to the Mekong River basin,

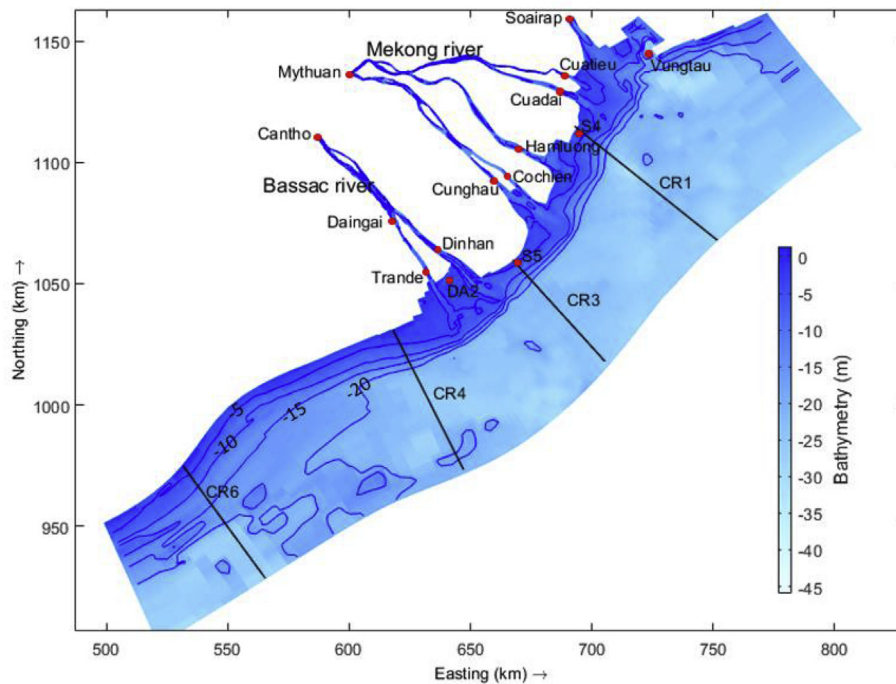


Fig. 1. Model coverage and boundary locations.

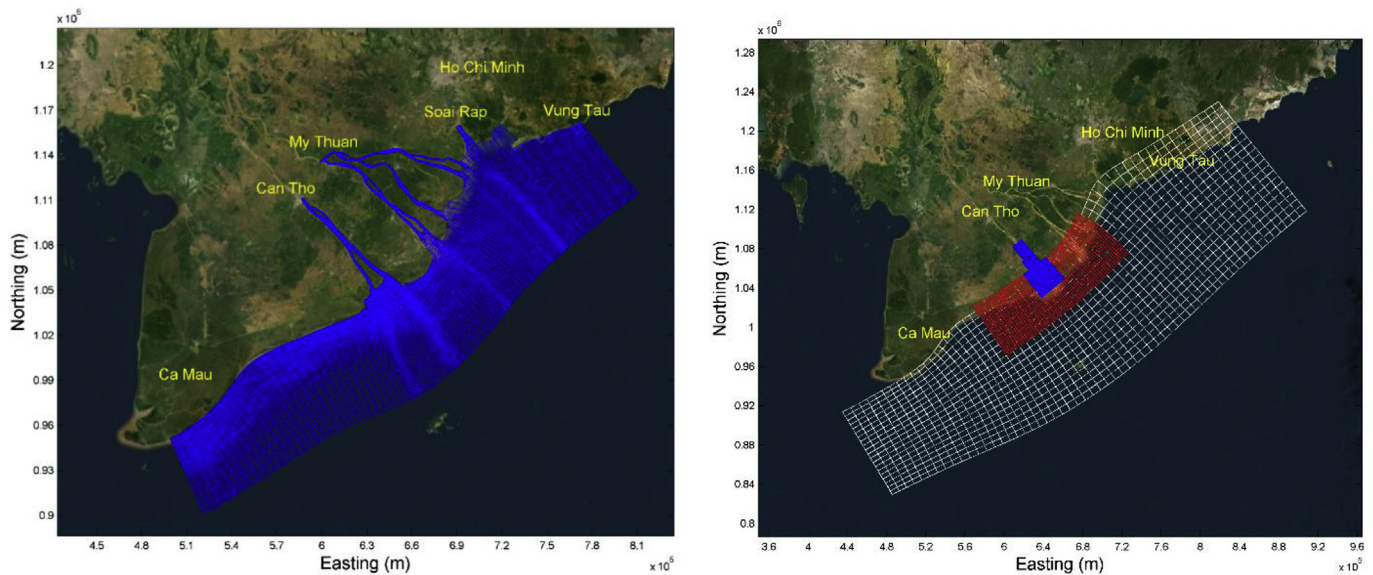


Fig. 2. Computational grid for Delft3D Flow (left) and three nesting grids for waves in the study area (white – the coarsest grid of 4–8 km of resolution; red – the moderate grid of 1.5–2.5 km of resolution; blue – the finest grid of 0.5–0.8 km of resolution) (right). (For interpretation of the references to colour in this figure legend, the reader is referred to the Web version of this article.)

so the use of a constant value may insignificantly impact on modeling results to a larger extent. Water level stations along the coast and inside the Bassac River such as Vung Tau, Vam Kenh, An Thuan, Ben Trai, Tra Vinh, Tran De, Dai Ngai and Can Tho were used for model calibration and validation (locations in Fig. 1). Currents data at DA2 (from 12–22 August 2009) and S5 (from 15–19 September 2009) were used for calibration in the flood season in 2009. Salinity data at Dai Ngai were collected from the Southern Regional Hydro Meteorological Centre. These data were measured from 01 to 19 April 2009 and from 26 March to 08 April 2010, and were used for calibration and validation, respectively.

Discharge data were measured simultaneously by an Acoustic Doppler Current Profiler (ADCP) device at seven estuaries (Cua Dai,

Cua Tieu, Ham Luong, Co Chien, Cung Hau, Dinh An, and Tran De as in Fig. 1) during the flood season from 15 to 30 September 2009. Wave and wind data were downloaded from the website of the European Centre for Medium-Range Weather Forecasts (ECMWF; the ERA Interim daily data). This dataset provided wave and wind field data in every 6 h from 1979 to 2016. The grid resolution was $0.5 \times 0.5^\circ$. For the study region (latitude from 7° to 11° and longitude from 104° to 109°), the wave and wind data during 2009–2010 were extracted at a point (8° , 107.5°) and were used to set up the wave model boundary.

3. Model setup

3.1. Set up of Delft3D-Flow model

3.1.1. Model coverage

The study area covered the two main rivers and sea domain. The Bassac River segment is from Can Tho to the sea, approximately 80 km, which includes the Tran De and Dinh An estuaries, influenced by tidal dynamics. The Mekong River segment is from My Thuan to the sea, about 95 km, which included the Cua Tieu, Cua Dai, Ham Luong, Co Chien and Cung Hau estuaries. We also modelled 20 km of the Soai Rap estuary, belonging to Sai Gon - Dong Nai, a neighboring river basin. The extension of the sea domain was approximately 340 km in the along-shore direction from Vung Tau to the Ca Mau Cape and 70 km in the cross-shore direction (Fig. 1).

3.1.2. Model grid

The 3D model used in this study consisted of a 2D horizontal grid that covered the model domain (see Fig. 2) along with a vertical grid that represents the third dimension. A curvilinear grid approach provides a high-resolution grid for the area of interests, for example, the Dinh An and Tran De estuaries and low resolution elsewhere. The model grid has a number of 25,004 cells (Fig. 2). The grid cell sizes vary from 100 to 9,841 m. For the vertical grid, 10 equidistant sigma layers were used.

3.2. Set up of Delft3D-Wave model

The computational grid of the wave model covered the whole flow model domain (see Fig. 2). For the simulation of wave propagation, three different scale and resolution computational grids were nested in order to focus on the river mouths. The largest scale grid covers approximately 505 km in the alongshore direction from Vung Tau to the Ca Mau Cape and 120 km in the cross-shore direction to the depth of 30–60 m, and the grid sizes varied from 4 to 8 km. This grid was used to calculate the offshore wave conditions at the outside boundaries of a finer wave grid located closer to the study area. The second computational grid was an intermediate grid with the grid sizes varying from 1.5 to 2.5 km, extending 150 km in the alongshore direction and 60 km in the cross-shore direction. This grid covered the Tran De, Dinh An, Cung Hau, Co Chien and Ham Luong estuaries. The final grid resolution varied from 0.5 to 0.8 km. The grid was approximately 30 km in the alongshore direction and expanded 57 km riverward from mouths to river upstream.

3.3. Parameterization

The 3D turbulence model used in this study was the K-Epsilon model. Considering the horizontal eddy viscosity and diffusivity, based on the calibration and given the relatively large scale of the model, the initial value was assigned as both $10 \text{ m}^2/\text{s}$ (Vinh et al., 2016). The calibrated bed roughness (Manning coefficients) value for hydrodynamic was obtained in the range of $0.016\text{--}0.023 \text{ m}^{-1/3}$. The averaged water temperature was set to $T = 27^\circ\text{C}$. Salinity conditions were set up for sea boundaries with value $S = 34 \text{ ppt}$ and $S = 0 \text{ ppt}$ for upstream river

boundaries.

Suspended sediments in the Mekong estuary are fine sand (non-cohesive) and silt (cohesive and flocculating material). The suspended sediment characteristics are spatially varying in the delta. Grain sizes are generally coarse in the upstream part and fine in the downstream areas. The median grain sizes are $15 \mu\text{m}$ in upstream and $3.9 \mu\text{m}$ in the downstream estuary and observed a floc size of $d_{50} \approx 40 \mu\text{m}$ of suspended sediment in the freshwater region of the estuary of the Bassac River (Hung et al., 2014a).

The bed composition was described by two fractions, a mud layer on the top and sand underlayer. On the top of bed composition is an initial mud layer of 2 cm. The bed composition in this study was described by a transport layer of 10 cm thickness, 20 layers of 10 cm thickness and a flexible underlayer. The sand layer was set up with an initial 2 m layer thickness and D_{50} of 0.11 mm. The $\tau_{cr,d}$ is assigned 1000 N/m^2 (continuous deposition), $\tau_{cr,e}$ is 0.2 N/m^2 , M is $2 \times 10^{-5} \text{ kg/m}^2/\text{s}$. Moreover, the sediment fall velocity (w_s) in fresh and salt water are 0.5×10^{-4} and $3.25 \times 10^{-4} \text{ m/s}$, respectively (Nowacki et al., 2015; Wolanski et al., 1996).

Due to the lack of sand transport measurements in the upstream reach of the estuaries, the model uses the equilibrium sand concentration and bed load transport at the upstream boundaries. Sand concentration at the offshore boundaries was also set to equilibrium values, as these boundaries located in sufficiently deep water far from the river channels.

3.4. Simulation scenarios

The Mekong Delta is subject to a large variety of natural forces and human interventions including upstream hydropower development, and sand extraction in the lower Mekong River (Arias et al., 2019; Hecht et al., 2019). We, therefore, consider four scenarios consisting of (a) baseline (BL) with a simulated period of 2009–2010 (see Fig. S2 in Appendix for forcing conditions), (b) upstream reduction of sediment (URS) reducing 50% sediment volume of baseline, (c) sand extraction (SE) which is deepened to -6 to 13 m on the main river tributaries and (d) combination of upstream reduction of sediment and sand extraction (URS+SE) as described in Table 1. We then used the same boundary conditions and replicate for a period of 10 years to investigate long-term sedimentation processes.

4. Model verification

4.1. Model calibration

The calibration was performed during 2 periods, including March–April 2009 (the low flow season) and September–October 2009 (the high flow season). Water levels were calibrated at 10 stations of Vung Tau, Cua Tieu, Cua Dai, Ham Luong, Co Chien, Cung Hau, Tran De, Dinh An, Dai Ngai, and Can Tho. Discharges were calibrated at 7 cross-sections (Cua Tieu, Cua Dai, Ham Luong, Co Chien, Cung Hau, Tran De, and Dinh An) which covered the seven main outlets of the Mekong River. To evaluate the performance of the hydrodynamic model for each different data type, we followed the model evaluation technique as in Moriasi et al. (2007). The Nash-Sutcliffe efficiency

Table 1
Simulation scenarios for sediment transport and sand extraction.

Notation	Scenarios	Description
BL	Sediment transport during 2009–2010	The simulation period of 1 June 2009 to 30 May 2010
URS	Upstream reduction of sediment	The sediment reduction at Can Tho and My Thuan is 50% compared to the baseline.
SE	Sand extraction	Main branches will be deepened to -6.0 to -13.0 m , the total volume of sand mining in the Bassac river was estimated $108.9 \text{ million m}^3$ and in the Mekong river was $281.6 \text{ million m}^3$.
URS+SE	Upstream reduction of sediment and sand extraction	Combination of upstream reduction of sediment and sand extraction scenarios.

Table 2
Calibration results for water levels in the dry and flood seasons in 2009.

Stations	Dry season		Flood season	
	RSR	NSE	RSR	NSE
Vung Tau	0.128	0.984	0.136	0.982
Tran De	0.339	0.885	0.236	0.944
Dai Ngai	0.282	0.920	0.303	0.908
Can Tho	0.390	0.848	0.283	0.920
Co Chien	0.298	0.911	0.283	0.920
Ham Luong	0.238	0.943	0.214	0.954
Cua Dai	0.295	0.913	0.188	0.964
Cua Tieu	0.233	0.946	0.269	0.927

(NSE) was computed as shown in equation (1) and the relative squared error (RSE) is calculated as the ratio of the root mean square error (RMSE) and the standard deviation of the observation data (STDEV), as shown in equation (2):

$$NSE = 1 - \frac{\sum_{i=1}^n (Y_i^{obs} - Y_i^{sim})^2}{\sum_{i=1}^n (Y_i^{obs} - Y_i^{mean})^2} \quad (1)$$

$$RSE = \frac{RMSE}{STDEV_{obs}} = \frac{\sqrt{\sum_{i=1}^n (Y_i^{obs} - Y_i^{sim})^2}}{\sqrt{\sum_{i=1}^n (Y_i^{obs} - Y_i^{mean})^2}} \quad (2)$$

where: Y_i^{obs} is the i th observation for the constituent being evaluated; Y_i^{sim} is the i th simulated value for the constituent being evaluated; Y^{mean} is the mean of observed data for the constituent being evaluated, and n is the total number of observations.

Results from model calibration show a high agreement between observed and simulated data in terms of phase and amplitude (Table 2, Figs. S2–S4 and Table S1 in Appendix for model performance evaluation). In this study, we considered both water levels and discharges to evaluate the performance of the hydrodynamic model because of the complicated geographical and geometrical features of the Mekong estuaries. Besides water levels, the assessment of the gauged discharge was important in the case of the Mekong model because the tidal wave propagates through the whole model domain reaching and significantly affecting the discharge model boundaries (Dang et al., 2018a).

To calibrate suspended sediment concentration (SSC) of the model, we compared with in-situ data, which were collected at seven stations

of Cua Tieu, Cua Dai, Ham Luong, Co Chien, Cung Hau, Dinh An and Tran De during September and October 2009 by SIWRR. Fig. 3 shows that most SSC simulations agreed with observations, although the errors for amplitude and phase at the Tran De station are variable. The reason is that the observed samples are very sporadic, so that some peaks of simulation could not be compared because of missing observation data.

4.2. Model validation

4.2.1. Salinity validation

This section presents comparisons between the simulated and observed salinity time series from 01 to 19 April 2009 and from 26 March to 08 April 2010. In general, there was a good agreement in terms of trends and amplitudes of depth-average salinity concentration in both the dry season 2009 and 2010 (Figs. S6–S7 and Table S2 in Appendix). The range of salinity intrusion during the dry season (around 50 km) is consistent with those observed at the Co Chien estuary as in Gugliotta et al. (2017). The model prediction underestimated salt concentration in 2010 because this was a critical year in 60-year records.

4.2.2. Wave validation

The wave and flow modules are coupled to simulate hydrodynamic processes and wave propagation. Fig. S8 presents wave height validation results at the DA2, S4 and S5 stations. When the differences between observation and simulation were acceptable, the general trends of the simulations were reasonably in agreement with observations, given that the offshore boundary conditions were based on a large-scale global model.

4.2.3. Suspended sediment validation

To validate the spatial variability of the modelled SSCs, we used satellite images which were collected from the project “Kalicôtier, ACRI-ST” during 2009–2010 (https://www.acri-st.fr/). The spatial resolution of the products was 300 × 300 m. We compared the numerical results with a set of 12 satellite images, one for every month of simulation. Thus, we can validate features related to sediment plumes in the Mekong estuaries and coastal regions in the both high flow and low flow seasons derived from modeling and satellite imagery.

Fig. 4 and Fig. S9 – S11 (in Appendix) shows simulated SSC patterns (top panel) which is rather similar to the satellite images (bottom panel). The highest SSC values were observed at the estuaries in September–November 2009 when the river discharge and SSC values of the

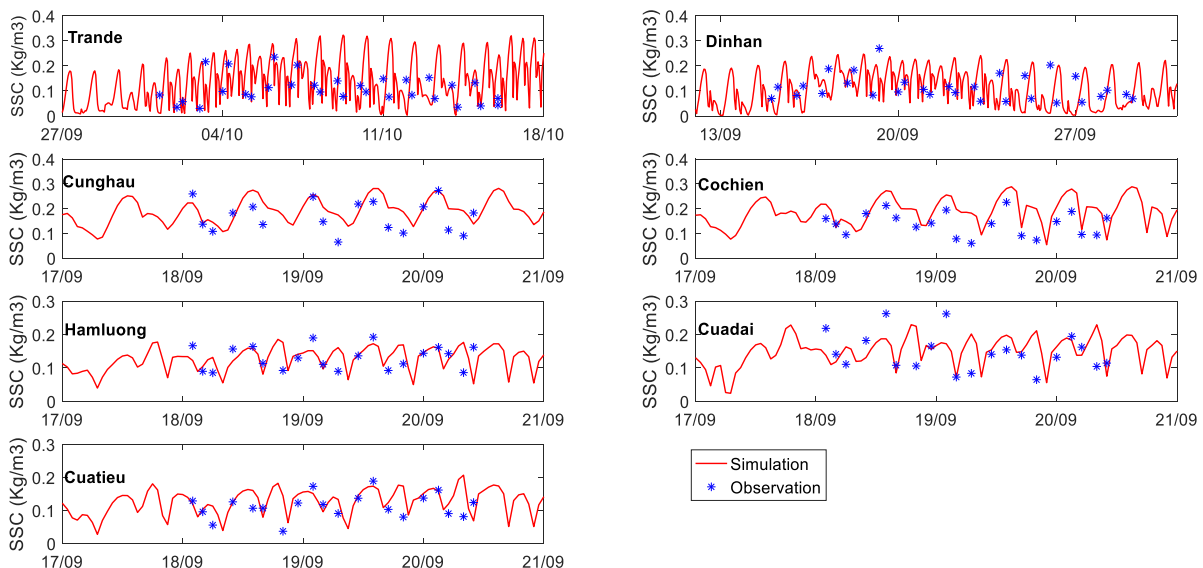


Fig. 3. Model calibration results for SSC at seven stations during the flood season in 2009.

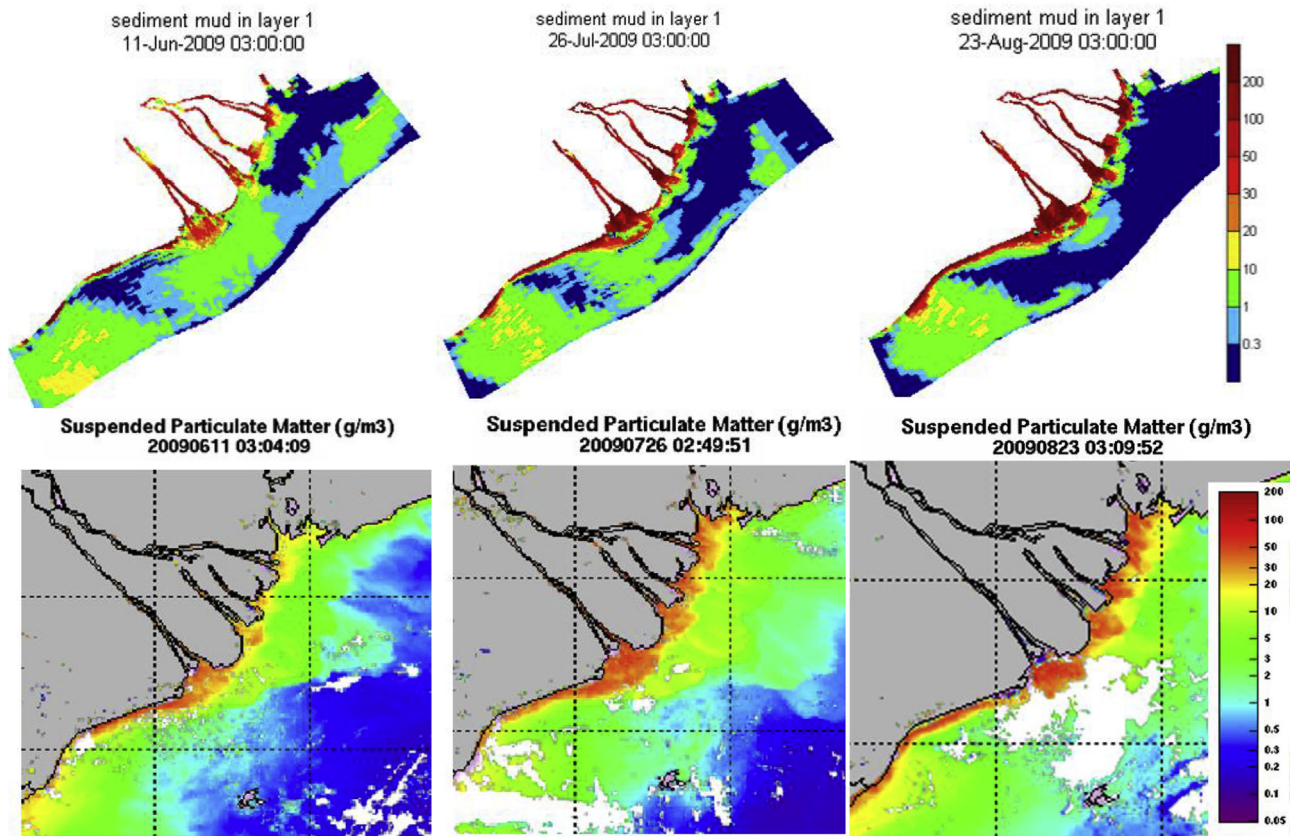


Fig. 4. Comparison of SSC distribution in the study area between simulation (top panels) and satellite image (bottom panels) in June, July and August 2009.

Mekong River were high. During these months, sediment plumes were formed in the river mouths (Fig. 4 and Figs. S9–S11). Wind and wave directed the plumes to south-westward along the coast. During the dry season, the sediment plume propagated from the river mouths to the south boundary along the coastline. Overall, we could conclude that the model represented successfully the essential features of the seasonal behaviors of SSC.

4.2.4. Validation of the long-term morphodynamical approach

To validate the approach with morphological acceleration, results from the first morphological year using Morfac (Morphological Acceleration Factor) of 25 were compared with those without acceleration and Morfac of 1. Fig. 5 showed that the erosion and deposition patterns of the Morfac 25 simulation were very similar to those of the baseline case. The only difference is less deposition on the edge of delta shields with Morfac. Therefore, this method could be used to simulate a period of 10 years.

5. Results and discussion

5.1. Sediment balance

We found that the distribution of mud and sand was highly variable between the estuaries. We extracted cumulative suspended sediment transport at the cross sections at Dinh An and Tran De on the Bassac river and Cua Tieu, Cua Dai, Ham Luong, Co Chien and Cung Hau on the Mekong river. For longshore transport, we also extracted cumulative sediment at four cross-shore transects which were CR1, CR3, CR4 and CR6. The locations of the transects are presented in Fig. 1. Fig. 6 and Table S3 shows the cumulative suspended sediment transport (both mud and sand) at the seven cross sections in the Mekong and Bassac estuaries from June 2009 to May 2010. At the large estuaries such as

Dinh An, Tran De, Co Chien and Cung Hau, we found that the volume of suspended mud is two times higher than that of suspended sand transported. However, at the smaller estuaries such as Cua Tieu, Cua Dai and Ham Luong, the volume of suspended mud was lower than suspended sand. The reduced shear stress at the tidal river – estuary interface of the small estuaries causes mud deposition described in McLachlan et al. (2017) may be the main reason of this phenomenon.

In general, almost all sediment was flushed to the sea during the high river flows of the flood season (August to November) while in the dry season, sediment supplies to the sea reduced rapidly. Fig. 7 shows the cumulative sediment transport (both suspended and bedload) at the seven cross sections at the estuaries of the Mekong and Bassac rivers from June 2009 to May 2010. In some estuaries, sediment flowed back into the river system such as Dinh An and Tran De (the Bassac river) and Cua Dai, Ham Luong, Co Chien and Cua Dai (the Mekong river). This was consistent with Nowacki et al. (2015) in which they found a similar trend at the Dinh An estuary.

Due to the seasonal characteristics of sediment transportation, almost 90% of sediment at the inlets (Can Tho and My Thuan) was washed out to the sea. At the Dinh An and Tran De estuaries on the Bassac River, sediment was exported to the sea at approximately 5.0 million m^3 in the flood season in 2009, and only 0.5 million m^3 imported to the delta in the dry season in 2010. Totally, the sediment exported to the sea from the Bassac branches was approximately 4.5 million m^3 during the simulation period, in which Dinh An and Tran De contributed 3.0 million m^3 (67%) and 1.5 million m^3 (33%), respectively. While Nowacki et al. (2015) estimated suspended sediment exported yearly to the sea at 11 million ton/year at Dinh An, this value is higher than in our study (8 million tons at Dinh An) during 2009–2010. In the Mekong River system (including the Cua Tieu, Cua Dai, Ham Luong, Co Chien and Cung Hau estuaries), the cumulative sediment amount to the sea reached approximately 4.2 million m^3 , in which the Co Chien and Cung

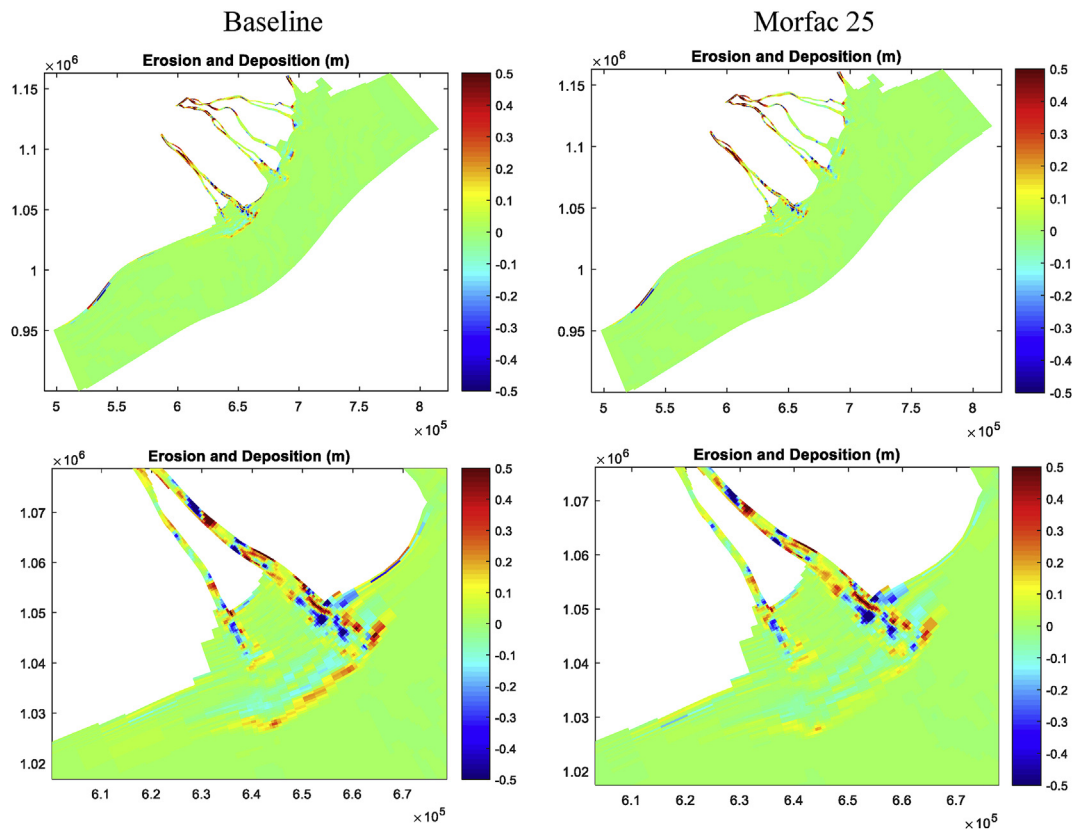


Fig. 5. The erosion and deposition after a year simulation for whole domain (up panel) and the estuaries of the Bassac River (bottom panel) for the baseline (left) and Morfac 25 (right).

Hau estuaries contributed 3.0 million m³, accounting for 72%, while the others contributed 1.2 million m³, and accounted for 28%.

5.2. Annual behavior

Modeling showed a significant amount of sediment discharged through the Mekong river system. We calculated that the cumulative suspended sediment discharge through Can Tho and My Thuan for 12

months (June 2009 to May 2010) is estimated about 66.0 million ton. Manh et al. (2014) used a 1-D model and found that an amount of 25.9–42.0 million ton of sediment flowed through Can Tho and My Thuan in 2009–2010. This estimate, however, is smaller than in our study because Manh et al. (2014) focused rather on the floodplains of the Vietnamese Mekong Delta and their model was calibrated for upper stations. Meanwhile, the ratios of sediment of the Bassac and Mekong branches exported to the sea in the flood season were 46% and 54%

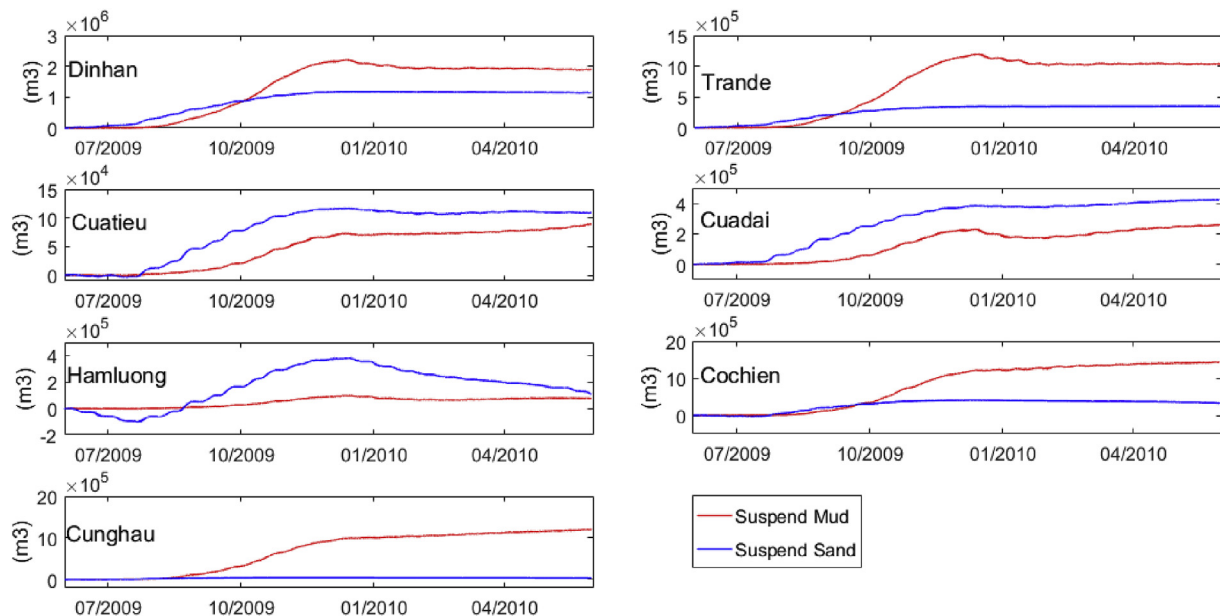


Fig. 6. Cumulative suspended mud and sand transport through the river mouths of the Mekong River in 2009–2010.

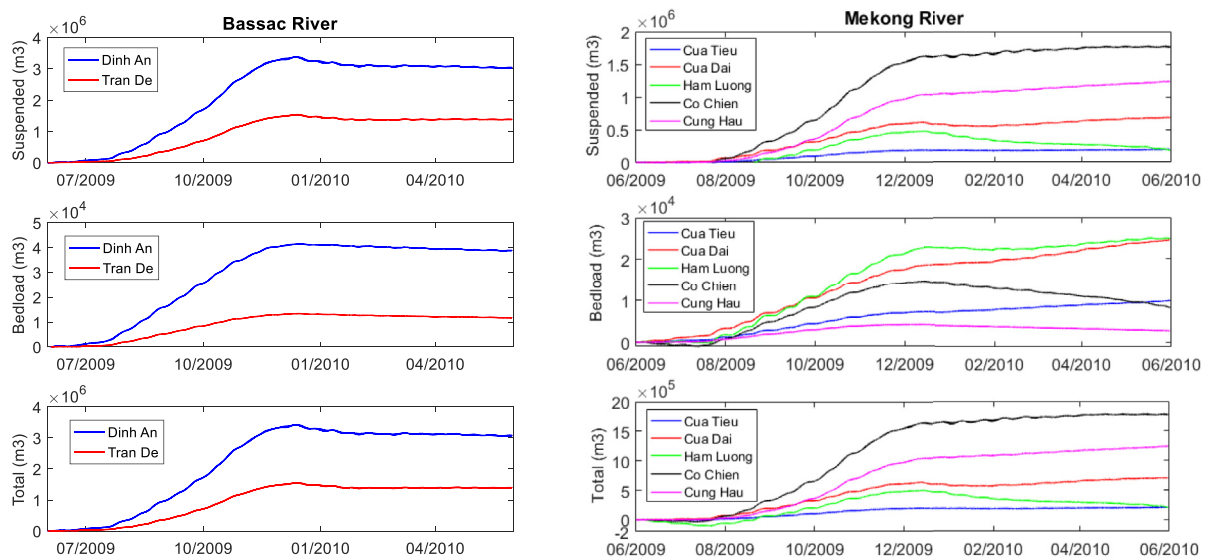


Fig. 7. Cumulative suspended sediment transport at the seven Bassac and Mekong estuaries in 2009–2010.

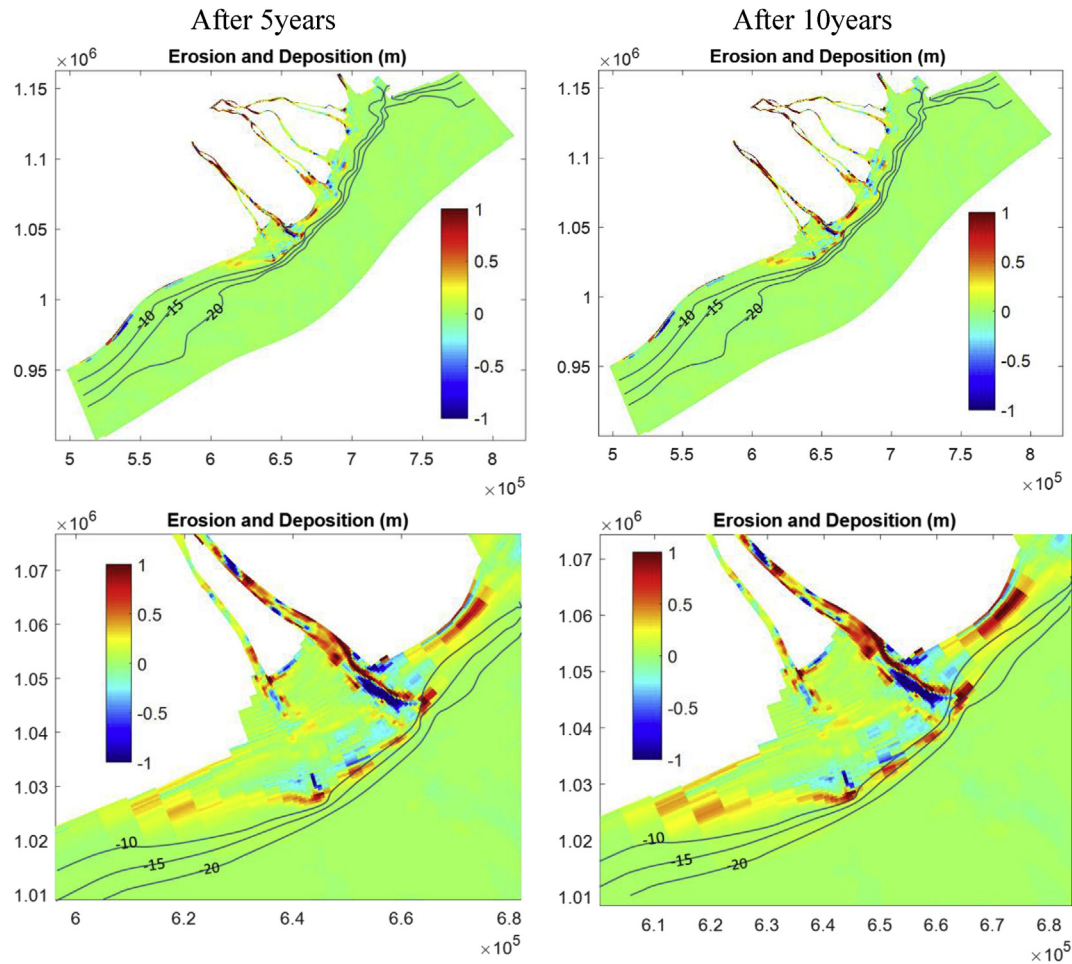


Fig. 8. Morphological changes of the Mekong coast (upper panel) and Bassac estuary (lower panel) after 5 and 10 years of simulation.

respectively, and these values are consistent with the rates calculated by Manh et al. (2014).

The morphodynamic simulation demonstrated a complex evolution of the coastal zone of the Mekong Delta. In the estuarine regions, erosion and deposition occurred alternatively. However, in the south-west

coastal region (east of the Ca Mau cape and coastal Ganh Hao), erosion dominated. This result was in line with the study by Anthony et al. (2015, 2017). Fig. 8 displays clearly erosion and deposition processes at the Bassac estuaries. Deposition processes occurred mainly at the Dinh An and Tran De mouths and in front of the Bassac estuaries. Moreover,

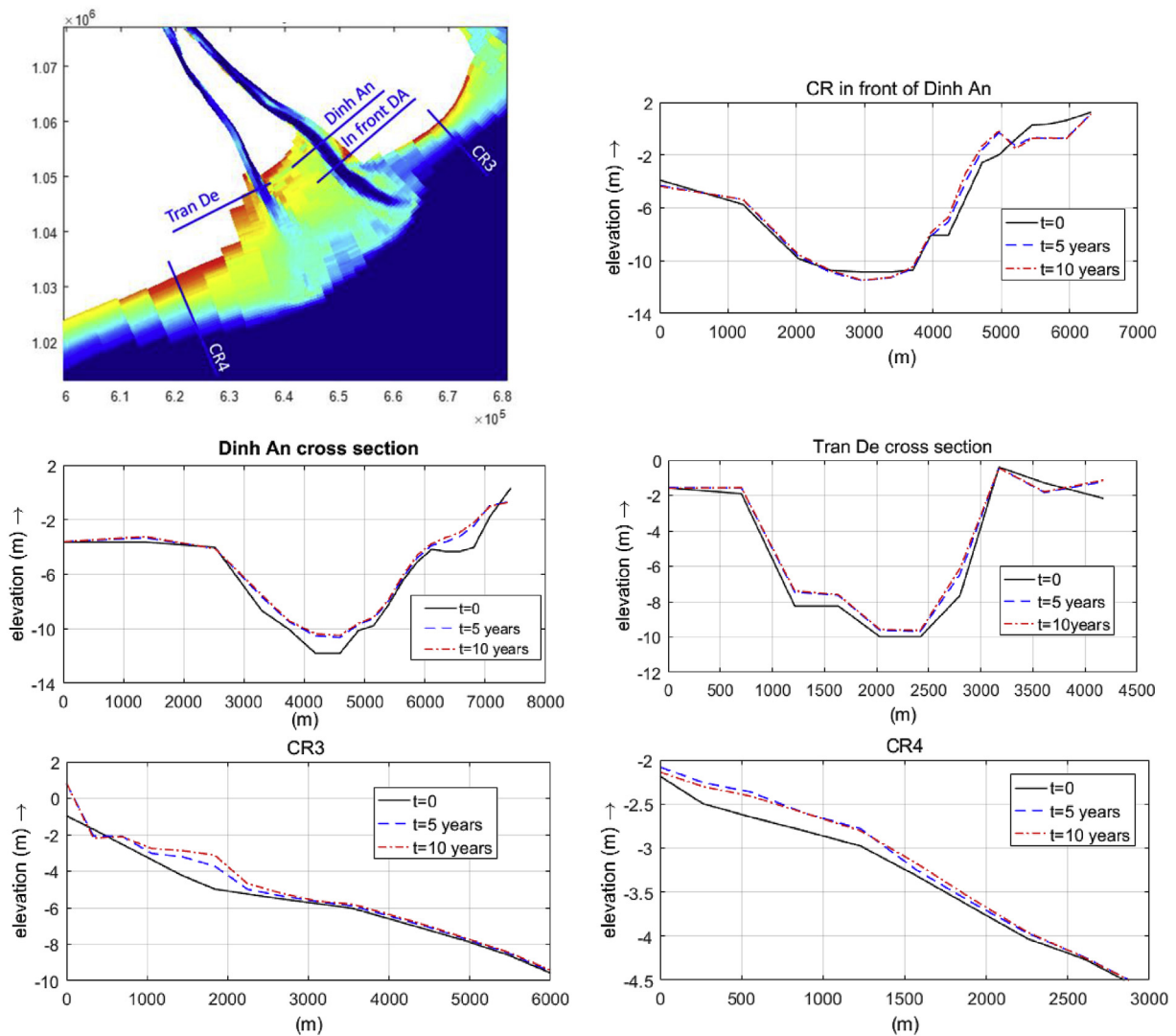


Fig. 9. Changes in cross section profiles after 5- and 10-years simulation.

the deposition processes seem to be dominant in front of Cu Lao Dung (between the Dinh An and Tran De estuaries) during the time of simulation while erosion prevailed at a channel in front of the Dinh An mouth. These erosion activities could form a new channel in the future.

Modeling results show offshore barrier formation in front of the estuaries was due to the massive deposition of river sediments out of the Mekong River. During the flood season, large sediment loads can be expected to form seaward shoals around the river mouths. This phenomenon may initiate barrier formation in front of the Bassac estuaries; these bars developed and migrated to the southwest of the Bassac estuaries after 1, 5 and 10 years of simulation. At the same time, bars were also formed at the north-east of the Bassac estuaries (Fig. 8); these bars developed and migrated to southwest by waves and long-shore currents during the north-east monsoon, which creates spits on the left of the Dinh An mouth, these trends agreed with the study by Xing et al. (2017). Fig. 9 presents cross-sectional changing after 5- and 10-year simulation at the Bassac estuaries. The cross sections of Dinh An, CR in front Dinh An and Tran De showed clear bathymetry changes in the 5-year timeframe, but these cross sections became almost stable after 5 years. Deposition occurs at the cross sections of the Dinh An and Tran De mouths. However, at the same time erosion took place at the riverbed of the cross section in front of Dinh An. Data analysis for the CR3 and CR4 cross sections show that sediment strongly deposited in

the range from the coastal line to 2.5 km offshore. As a result, the bars were formed in shallow water in this range. The changes in depth profiles found in this study is also in-line with what obtained by a two year in-situ measurement in Tamura et al. (2010). Via remote sensing data analysis, these trends were also discussed in Xing et al. (2017), Tanaka et al. (2012, 2016) and Anthony et al. (2015). It is important to notice that there an asymmetric long-term erosion and deposition at the river mouths. This causes by the differences in river discharges, net sediment transport, and the currents as mentioned above and in Ogston et al. (2017).

5.3. SSC distribution

We evaluated the distribution of SSC at the surface layer for the four management scenarios in the flood season and the dry season. Fig. 10 presents SSC distribution in the flood season after 9 years of simulation. The BL scenario had the highest surface SSC values both in the rivers and along the coastal zone compared to the other scenarios. In contrast, the lowest SSC values at the top layer were observed in the URS+SE scenario. Both sand extraction at the lower Mekong basin and SSC reduction due to upstream water infrastructure development could reduce significantly spatial SSC distribution as well as the amplitude of sediment concentration in the delta and along the coast in the wet and dry season. It is very clear that sediment distribution reduced

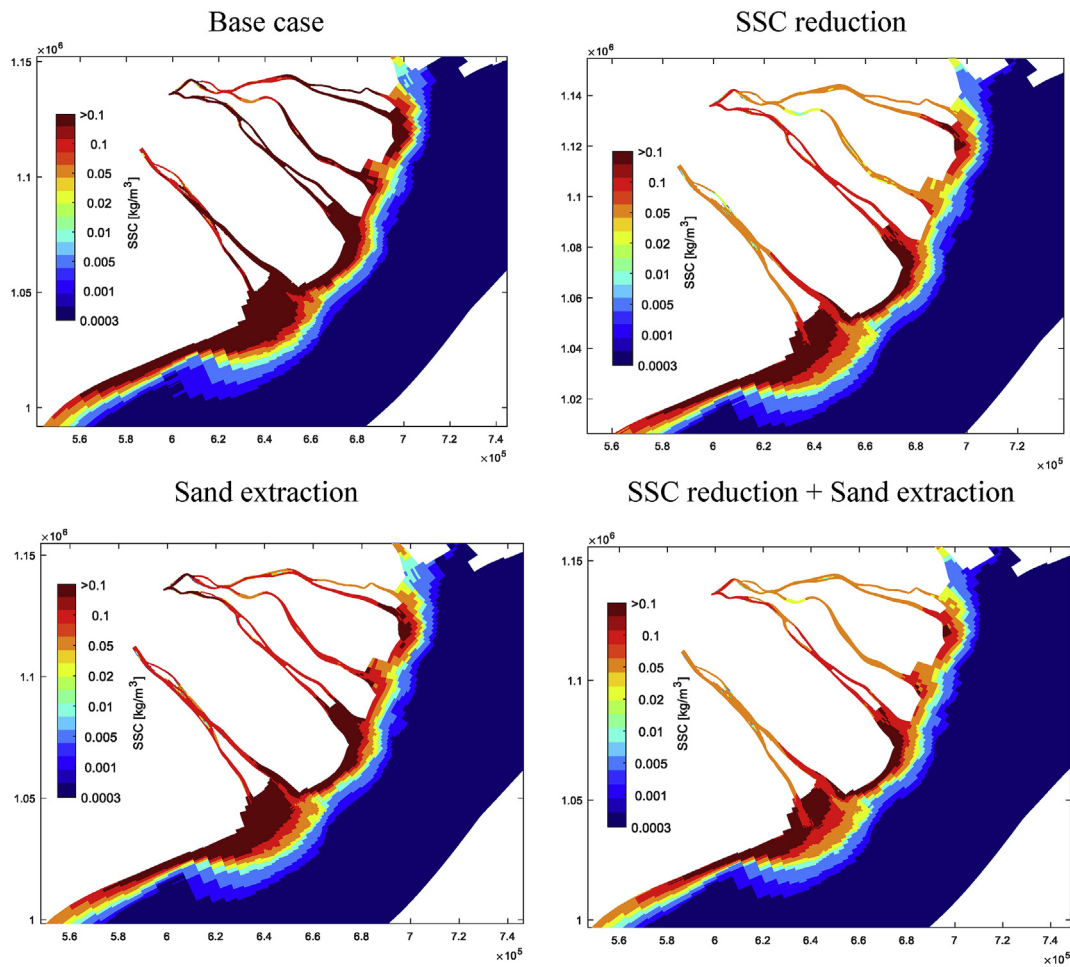


Fig. 10. The mean SSC distribution in the flood season after 9 years simulation.

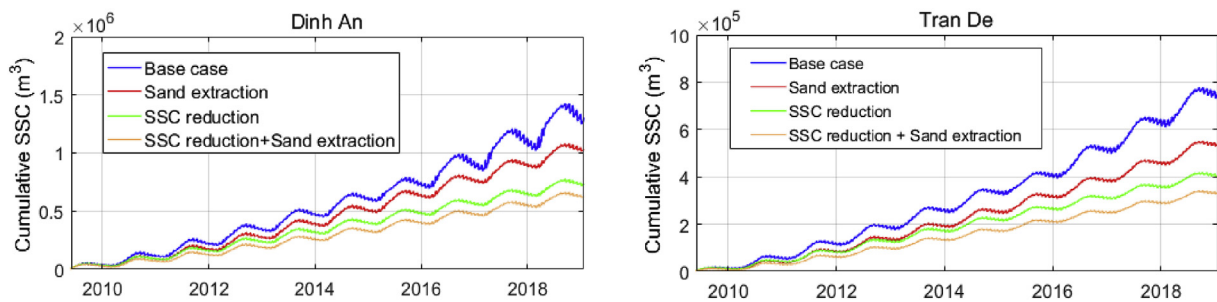


Fig. 11. Cumulative sediment transport amounts at the Dinh An and Tran De cross sections after 10-years simulation.

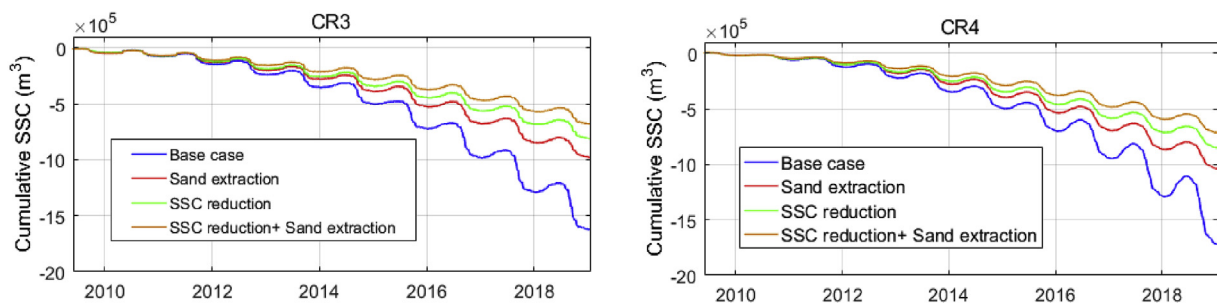


Fig. 12. Cumulative sediment transport at the CR3 and CR4 cross sections after 10-years simulation.

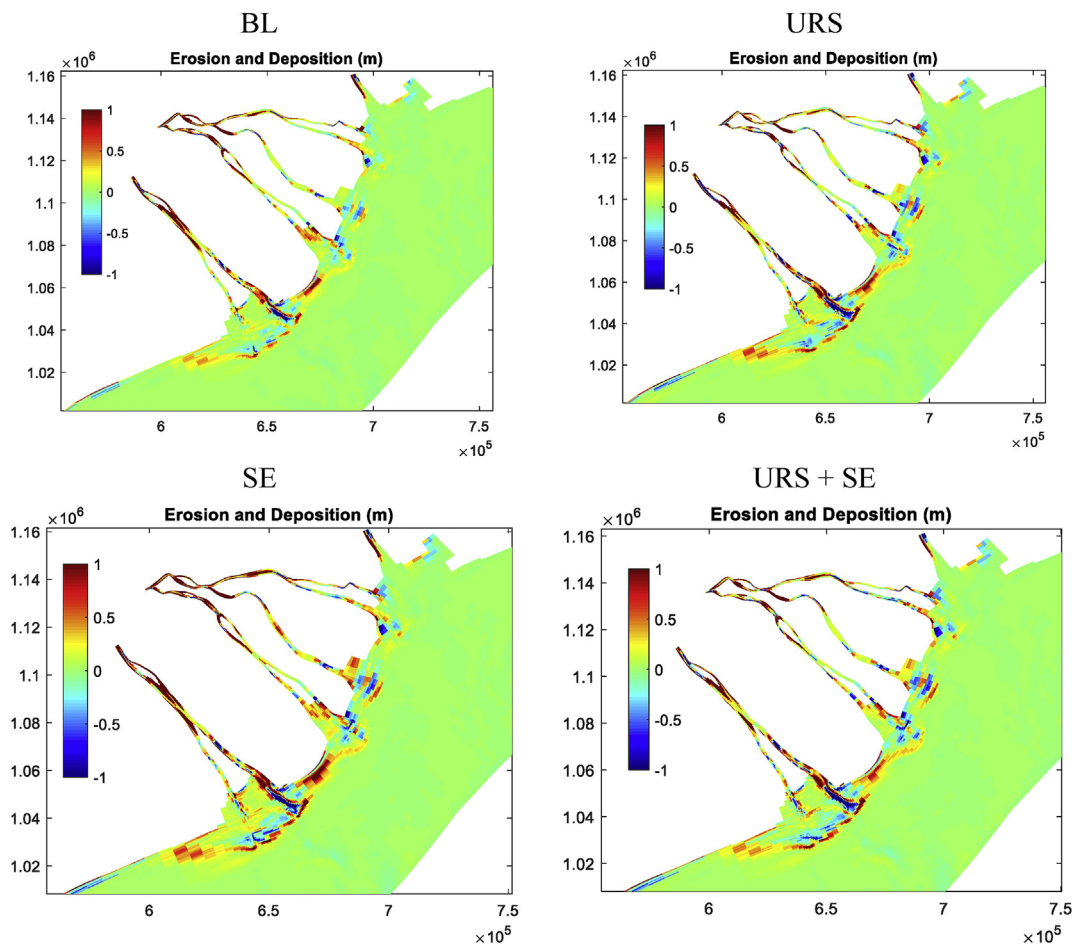


Fig. 13. Erosion and deposition in the four scenarios after 10-years simulation.

significantly near the coast and in the estuaries. Especially, the coastal areas between the Ham Luong and Dinh An estuaries and the south of Dinh An and Tran De, SSC reduced more than 50% while in other areas SSC reduced about 20% compared to the base case. Between these two scenarios, the sand extraction scenario impacted less on SSC reduction than upstream development.

Sand extraction at the main branches in the lower Mekong river and upstream SSC reduction also strongly affected sediment supplied to the sea. SSC reduced significantly by about 50% compared to the base case. Among these scenarios, in term of the amount of SSC to the sea, the URS + SE scenario was the most severe scenario, and it was influenced relatively less in the SE scenario. The modification in sediment discharged to the sea indicates that the sedimentation and erosion processes at the estuaries may change. The process of the seaward expansion of the Mekong Delta would slow down as a result or turn into recession. Fig. 11 describes SSC delivered to the sea via the Dinh An and Tran De cross sections at the Bassac estuaries for four scenarios. Though the Mekong Delta is very young compared to other river deltas around the world (Ta et al., 2002; Tamura et al., 2012), it has been pushed to the degradation phase due to human intervention.

The cumulative SSC transport along the coast also reduces significantly (see Fig. 12 and Table S4 for SSC at the CR3 and CR4 cross sections) between the base case and the other scenarios (positive values mean the north-east direction transportation; negative values mean the south-west direction transportation). SSC transported along the coast to the south area in the SSC reduction + Sand extraction scenario (URS + SE) reduced to less than half compared to the base case. Consequently, less sediment supply will be delivered to the southwest delta area including the Ca Mau Cape; as a result, this area may be expected

to experience reduced accretion and increased erosion.

5.4. Long-term sedimentation and erosion patterns

Generally, there were similar trends in the spatial patterns of erosion and deposition for four scenarios after 10-years simulation: erosion and deposition in the river, bars forming in front of the estuaries and prevailing erosion in the south-west coast (Fig. 13). However, there were differences between the baseline scenario and the others, for instance, more erosion can be found over the study area in other scenarios compared to the baseline. Strong erosion occurred in front of the estuaries and in the river branches near the mouths regardless of the scenarios. Compared to the baseline (BL), in the other three scenarios, bar formation in front of the estuaries seems more pronounced. This is because the bars were pushed offshore due to the more concentrated flow in the channels, which appears as a result of erosion and sedimentation patterns.

The Mekong delta was formed by the dynamic interaction of fluvial sediment supply and the redistribution of sediment by coastal processes. The changing conditions at upstream rivers, such as SSC reduction and sand mining in the main branches downstream significantly affected the erosion and deposition processes in the estuary mouths, both in intensity and spatial patterns. As a result, major effects on the coastal morphology may be expected.

In this study, we did not model localized and subsoil processes. In further studies, the effect of mangrove forests along the coast should be considered in the model to understand the mechanisms of sediment trapping in the vegetation. In addition, the subsidence in the Mekong delta and sea level rise are likely to further affect the morphological

evolution of the shelf and coastal areas.

6. Conclusions

The estuaries and coastal zone processes of the Mekong Delta were investigated with a well-calibrated Delft-3D model. We found that at the river mouths, seasonal sediment transport is strongly modulated by river discharges and monsoons. When sand-mud sedimentation processes are related to seasonal river discharges, the direction of suspended sediment movement depends on the direction of the monsoon. The ratio between sand and mud also varies at each estuary, depending on its hydraulic condition. The sediment transport alongshore is dominant during the north-east monsoon, especially in November, December and January.

The results of the long-term morphodynamics in 10-years simulation show the erosion and deposition processes in the estuaries and the coast. In the estuaries region erosion and deposition occurred alternately; bars were formed in front of the estuaries, then these bars developed and migrated to the south-west region. Significant erosion processes occurred in the eastern of the Ca Mau cape, in accordance with locations of observed coastline retreat.

Human activities such as sand mining and hydropower development in the Mekong basin reduced sediment transport from the river to the sea and longshore, thereby changing the erosion and deposition processes in the estuaries. These human-induced processes caused the delta to develop more slowly or leads to recession. Further actions such reducing sand mining or dam operation should be studied to ensure the delta to develop sustainably.

Conflicts of interest

The authors declare no conflict of interest.

Author contributions

L.X.T. designed the study, processed and analyzed the data, developed the models, interpreted the results and wrote the paper. V.Q.T. and S.P.V provided data, assisted in the data analyses and drafting the manuscript and D.T.A and T.D.D created first manuscript and finalized the final version. The manuscript has been carried out together by all authors, who contributed to the model development stage with theoretical considerations and practical guidance, assisted in the interpretations and integration of the results and helped in preparation of this paper with proof reading and corrections.

Acknowledgement

The authors would like to thank Southern Institute of Water Resource Research Ho Chi Minh city for providing most of the data. Simulations were carried out on the Dutch national e-infrastructure with the support of the SURF Cooperative. V.Q.T., J.R. and D.R. were supported by the ONR Tropical Deltas DRI under grant N00014-15-1-2824. The authors would like to thank the editors and anonymous reviewers for their comments which help us to improve the quality of this manuscript significantly.

Appendix A. Supplementary data

Supplementary data to this article can be found online at <https://doi.org/10.1016/j.csr.2019.07.015>.

References

Anthony, E.J., Brunier, G., Besset, M., Goichot, M., Dussouillez, P., Nguyen, V.L., 2015. Linking rapid erosion of the Mekong River Delta to human activities. *Sci. Rep.* 5, 14745. <https://doi.org/10.1038/srep14745>.

- Anthony, E.J., Dussouillez, P., Dolique, F., Besset, M., Brunier, G., Nguyen, V.L., Goichot, M., 2017. Morphodynamics of an eroding beach and foredune in the Mekong River delta: Implications for deltaic shoreline change. *Cont. Shelf Res.* 147, 155–164. <https://doi.org/10.1016/j.csr.2017.06.018>.
- Arias, M.E., Holtgrieve, G.W., Ngor, P.B., Dang, T.D., Piman, T., 2019. Maintaining perspective of ongoing environmental change in the Mekong floodplains. *Curr. Opin. Environ. Sustain.* 37, 1–7.
- Dang, D.T., Cochrane, T.A., Arias, M.E., Dang, V.P., 2018a. Future hydrological alterations in the Mekong Delta under the impact of water resources development, land subsidence and sea level rise. *J. Hydrol. Reg. Stud.* 15, 119–133. <https://doi.org/10.1016/j.ejrh.2017.12.002>.
- Dang, T.D., Cochrane, T.A., Arias, M.E., 2018b. Quantifying suspended sediment dynamics in mega deltas using remote sensing data: a case study of the Mekong floodplains. *Int. J. Appl. Earth Obs. Geoinf.* 68, 105–115.
- DeMaster, D.J., Liu, J.P., Eidam, E., Nittrouer, C.A., Nguyen, T.T., 2017. Determining rates of sediment accumulation on the Mekong shelf: timescales, steady-state assumptions, and radiochemical tracers. *Cont. Shelf Res.* 147, 182–196.
- Duong, T.M., Ranasinghe, R., Luijendijk, A., Dastgheib, A., Roelvink, D., 2012. Climate change impacts on the stability of small tidal inlets: a numerical modelling study using the realistic analogue approach. *Int. J. Ocean Clim. Syst.* 3, 163–172. <https://doi.org/10.1260/1759-3131.3.3.163>.
- Egbert, G.D., Erofeeva, S.Y., 2002. Efficient inverse modeling of barotropic ocean tides. *J. Atmos. Ocean. Technol.* 19, 183–204.
- García, M., Ramirez, I., Verlaan, M., Castillo, J., 2015. Application of a three-dimensional hydrodynamic model for San Quintin Bay, B.C., Mexico. validation and calibration using OpenDA. *J. Comput. Appl. Math.* 273, 428–437. <https://doi.org/10.1016/j.cam.2014.05.003>.
- Gugliotta, M., Saito, Y., Nguyen, V.L., Ta, T.K.O., Nakashima, R., Tamura, T., Uehara, K., Katsuki, K., Yamamoto, S., 2017. Process regime, salinity, morphological, and sedimentary trends along the fluvial to marine transition zone of the mixed-energy Mekong River delta, Vietnam. *Cont. Shelf Res.* 147, 7–26.
- Hecht, J.S., Lacombe, G., Arias, M.E., Duc, T., 2019. Hydropower dams of the Mekong River basin: a review of their hydrological impacts. *J. Hydrol.* 568, 285–300. <https://doi.org/10.1016/j.jhydrol.2018.10.045>.
- Heege, T., Kiselev, V., Wettle, M., Hung, N.N., 2014. Operational multi-sensor monitoring of turbidity for the entire Mekong Delta. *Int. J. Remote Sens.* 35, 2910–2926. <https://doi.org/10.1080/01431161.2014.890300>.
- Hein, H., Hein, B., Pohlmann, T., 2013. Recent sediment dynamics in the region of Mekong water influence. *Glob. Planet. Chang.* 110, 183–194. <https://doi.org/10.1016/j.gloplacha.2013.09.008>.
- Hung, N.N., Delgado, J.M., Güntner, A., Merz, B., Bárdossy, A., Apel, H., 2014a. Sedimentation in the floodplains of the Mekong Delta, Vietnam. Part I: suspended sediment dynamics. *Hydrol. Process.* 28, 3132–3144. <https://doi.org/10.1002/hyp.9856>.
- Hung, N.N., Delgado, J.M., Güntner, A., Merz, B., Bárdossy, A., Apel, H., 2014b. Sedimentation in the floodplains of the Mekong delta, Vietnam Part II: deposition and erosion. *Hydrol. Process.* 28, 3145–3160. <https://doi.org/10.1002/hyp.9855>.
- Kondolf, G.M., Rubin, Z.K., Minear, J.T., 2014. Dams on the Mekong: cumulative sediment starvation. *Water Resour. Res.* 50, 5158–5169. <https://doi.org/10.1002/2013WR014651>.
- Lu, S., Tong, C., Lee, D.-Y., Zheng, J., Shen, J., Zhang, W., Yan, Y., 2015. Propagation of tidal waves up in Yangtze estuary during the dry season. *J. Geophys. Res. Ocean.* 120. <https://doi.org/10.1002/2014JC010632>.
- Manh, N.V., Dung, N.V., Hung, N.N., Merz, B., Apel, H., 2014. Large-scale quantification of suspended sediment transport and deposition in the Mekong Delta. *Hydrol. Earth Syst. Sci. Data* 18, 3033–3053. <https://doi.org/10.5194/hessd-11-4311-2014>.
- Manh, N. Van, Dung, N.V., Hung, N.N., Kumm, M., Merz, B., Apel, H., 2015. Future sediment dynamics in the Mekong Delta floodplains: impacts of hydropower development, climate change and sea level rise. *Glob. Planet. Chang.* 127, 22–33. <https://doi.org/10.1016/j.gloplacha.2015.01.001>.
- Marchesiello, P., Nguyen, N.M., Gratiot, N., Loisel, H., Anthony, E.J., San, D.C., Nguyen, T., Almar, R., Kestenare, E., 2019. Erosion of the coastal Mekong delta: Assessing natural against man induced processes. *Cont. Shelf Res.* 181, 72–89.
- McLachlan, R., Ogston, A., Allison, M., 2017. Implications of tidally varying bed shear stress and intermittent estuarine stratification on fine-sediment dynamics through the Mekong's tidal river to estuarine reach. *Cont. Shelf Res.* 147, 27–37.
- Milliman, J.D., Farnsworth, K.L., 2011. *River Discharge to the Coastal Ocean. A Global Synthesis.* Cambridge University Press, the UK.
- Moriassi, D.N., Arnold, J.G., Van Liew, M.W., Bingner, R.L., Harmel, R.D., Veith, T.L., 2007. Model evaluation guidelines for systematic quantification of accuracy in watershed simulations. *Trans. ASABE (Am. Soc. Agric. Biol. Eng.)* 50, 885–900. <https://doi.org/10.13031/2013.23153>.
- MRC, 2011. *Planning Atlas of the Lower Mekong River Basin.* Mekong River Commission.
- Nowacki, D.J., Ogston, A.S., Nittrouer, C.A., Fricke, A.T., Van, D.T.P., 2015. Sediment dynamics in the lower Mekong River: transition from tidal river to estuary. *J. Geophys. Res. Ocean* 120. <https://doi.org/10.1002/2014JC010632>.
- Ogston, A.S., Allison, M.A., Mullarney, J.C., Nittrouer, C.A., 2017. Sediment- and hydrodynamics of the Mekong Delta: from tidal river to continental shelf. *Cont. Shelf Res.* 147, 1–6. <https://doi.org/10.1016/j.csr.2017.08.022>.
- Roelvink, J.A., 2006. Coastal morphodynamic evolution techniques. *Coast. Eng.* 53, 277–287. <https://doi.org/10.1016/j.coastaleng.2005.10.015>.
- Ta, T., Nguyen, V., Tateishi, M., Kobayashi, I., Tanabe, S., Saito, Y., 2002. Holocene delta evolution and sediment discharge of the Mekong River, southern Vietnam. *Quat. Sci. Rev.* 21, 1807–1819. [https://doi.org/10.1016/S0277-3791\(02\)00007-0](https://doi.org/10.1016/S0277-3791(02)00007-0).
- Tamura, T., Horaguchi, K., Saito, Y., Nguyen, V.L., Tateishi, M., Ta, T.K.O., Nanayama, F., Watanabe, K., 2010. Monsoon-influenced variations in morphology and sediment of a

- mesotidal beach on the Mekong River delta coast. *Geomorphology* 116 (1–2), 1–23.
- Tamura, T., Saito, Y., Nguyen, V.L., Ta, T.O., Bateman, M.D., Matsumoto, D., Yamashita, S., 2012. Origin and evolution of interdistributary delta plains; insights from Mekong River delta. *Geology* 40 (4), 303–306.
- Tanaka, A., Uehara, K., Tamura, T., Saito, Y., Nguyen, V.L., Ta, T.K.O., 2016. Temporal changes in river-mouth bars from L-band SAR images: a case study in the Mekong River delta, South Vietnam. In: *Contributions to Modern and Ancient Tidal Sedimentology: Proceedings of the Tidalites 2012 Conference*, vols. 21–33 John Wiley & Sons, Chichester, UK.
- Tanaka, A., Uehara, K., Tamura, T., Saito, Y., 2012, July. Area change detection in river mouthbars at the Mekong River delta using Synthetic Aperture Radar (SAR) data. In: *2012 IEEE International Geoscience and Remote Sensing Symposium*, pp. 4911–4914.
- Thanh, V.Q., Reyns, J., Wackerman, C., Eidam, E.F., Roelvink, D., 2017. Modelling suspended sediment dynamics on the subaqueous delta of the Mekong River. *Cont. Shelf Res.* 147, 213–230. <https://doi.org/10.1016/j.csr.2017.07.013>.
- Unverricht, D., Nguyen, T.C., Heinrich, C., Szczuciński, W., Lahajnar, N., Stattegger, K., 2014. Suspended sediment dynamics during the inter-monsoon season in the subaqueous Mekong Delta and adjacent shelf, southern Vietnam. *J. Asian Earth Sci.* 79, 509–519. <https://doi.org/10.1016/j.jseas.2012.10.008>.
- van der Wegen, M., Jaffe, B.E., Roelvink, J.A., 2011. Process-based, morphodynamic hindcast of decadal deposition patterns in San Pablo Bay, California, 1856–1887. *J. Geophys. Res.* 116, 1–22. <https://doi.org/10.1029/2009JF001614>.
- Vinh, V.D., Ouillon, S., Van Thao, N., Ngoc Tien, N., 2016. Numerical simulations of suspended sediment dynamics due to seasonal forcing in the Mekong coastal area. *Water* 8, 255. <https://doi.org/10.3390/w8060255>.
- Wackerman, C., Hayden, A., Jonik, J., 2017. Deriving spatial and temporal context for point measurements of suspended sediment concentration using remote sensing imagery in the Mekong Delta. *Cont. Shelf Res.* 147, 231–245.
- Wolanski, E., Huan, N.N., Dao, L.T., Nhan, N.H., Thuy, N.N., 1996. Fine-sediment dynamics in the Mekong river estuary, Viet Nam. *Estuar. Coast Shelf Sci.* 43, 565–582.
- Wolanski, E., Nhan, N.H., Spagnol, S., 1998. Sediment dynamics during low flow conditions in the Mekong river estuary, Vietnam. *J. Coast. Res.* 14, 472–482.
- Xing, F., Meselhe, E.A., Allison, M.A., Weathers, H.D., 2017. Analysis and numerical modeling of the flow and sand dynamics in the lower Song Hau channel, Mekong Delta. *Cont. Shelf Res.* 147, 62–77. <https://doi.org/10.1016/j.csr.2017.08.003>.